Appl. Phys. B 80, 635–638 (2005)
DOI: 10.1007/s00340-005-1779-4

Applied Physics B
Lasers and Optics

S. TOKITA[1,✉]
J. KAWANAKA[1]
M. FUJITA[2]
T. KAWASHIMA[3]
Y. IZAWA[1]

Sapphire-conductive end-cooling of high power cryogenic Yb:YAG lasers

[1]Institute of Laser Engineering, Osaka University, 2-6 Yamadaoka, Suita, Osaka 565-0871, Japan
[2]Institute for Laser Technology, 2-6 Yamadaoka, Suita, Osaka 565-0871, Japan
[3]Central Research Laboratory, Hamamatsu Photonics K. K., 5000 Hirakuchi, Hamakita, Shizuoka 434-8601, Japan

Received: 6 January 2005 / Published online: 17 March 2005 •

ABSTRACT We have demonstrated a high-power laser oscillator with end-cooling using a sapphire-sandwiched Yb:YAG disk at near liquid nitrogen temperature. An output power of 75 W with a near-diffraction-limited beam was obtained from a 0.6-mm thick active medium. The slope efficiency and the maximum optical–optical efficiency were 80 and 70%, respectively, with respect to absorbed pump power.

PACS 42.55.Rz; 42.55.Xi

1 Introduction

The average power and the beam quality in solid-state lasers are limited by thermally induced effects such as thermal distortion, birefringence, or stress fracture in the solid-state laser medium. As one of the approaches to exceed the power limitation, operating the laser medium at cryogenic temperatures (<100 K) have been demonstrated in Yb:YAG lasers [1, 2] and Ti:sapphire lasers [3, 4]. This approach takes advantage of significant improvement of the material's thermal properties at low temperatures such as higher thermal conductivity, lower temperature coefficients of refractive index (dn/dT), and lower thermal expansion [5–8]. In the case of Yb-doped lasers, the cryo-cooling provides further advantages. In the lower temperature than about 100 K, the Yb-doped lasers such as Yb:YAG or Yb:YLF become the four-level lasers, and consequently the laser threshold is greatly reduced [9, 10]. In addition, the emission cross section increases because of fluorescence line narrowing [9, 11]. As the other approaches, cooling configurations to avoid the thermally induced effects have been demonstrated such as zigzag slab lasers and thin-disk lasers. The thin-disk laser concept introduced by Giesen et al. [12] allows one-dimensional heat flow in longitudinal direction and very high pump power densities without significant temperature rises, and provides good scalability. High power thin-disk lasers have been demonstrated with Yb:YAG and Yb:KYW oscillators [13–15]. Due to the thin-disk configuration which requires very thin active medium (typically 100–300 μm), multipass pumping scheme with complicated optics has been employed in many cases, where one face of the disk is used for pumping and lasing, and cooling is performed only from the other face.

Conduction cooling at both faces of thin-disk laser medium will enable to keep a lower temperature. Such cooling can be achieved by applying a highly thermal-conductive optical-transparent material as cooling media. Longitudinal cooling with transparent media has been demonstrated in end-pumped Nd:YAG lasers with undoped ends [16, 17]. Sapphire crystals had been adopted for Nd:YVO_4 and Nd:YAG lasers due to their higher thermal conductivity than the active media [18, 19]. Cryo-cooled sapphire crystal has an extremely high thermal conductivity and excellent optical properties. At 77 K, for example, sapphire's thermal conductivity is about 1000 W/m K, which is one order of magnitude higher than that of YAG crystals [5, 6]. A combination of thin-disk material and sapphire cooling media at cryogenic temperatures will extremely reduce the thermal effects. That enables one not only to increase the power limitation but also to employ a simple pump scheme without large pass numbers by using a thicker active media.

In this paper, we present a diode-end-pumped Yb:YAG disk laser with the conduction cooling from both faces using sapphire crystals operating in near liquid nitrogen temperature. High cw output power of 75 W with near-diffraction-limited beam was obtained from a 25-at.% doped 0.6-mm thick active medium. The peak temperature in the active medium was estimated by numerical simulations.

2 Experimental setup

A schematic diagram of our diode-pumped oscillator with a liquid-nitrogen-cooled Yb:YAG crystal is shown in Fig. 1. The plano-concave cavity consisted of a flat output coupler, a flat dichroic mirror and a concave high reflector with 5-m curvature. The total cavity length was 91 cm. The distance between the laser crystal and the output coupler was 75 cm. The laser crystal was 25-at.% Yb:YAG (Scientific Materials Corp.) with a 0.6-mm thickness

✉ Fax: +81-6-68774799, E-mail: stokita@ile.osaka-u.ac.jp

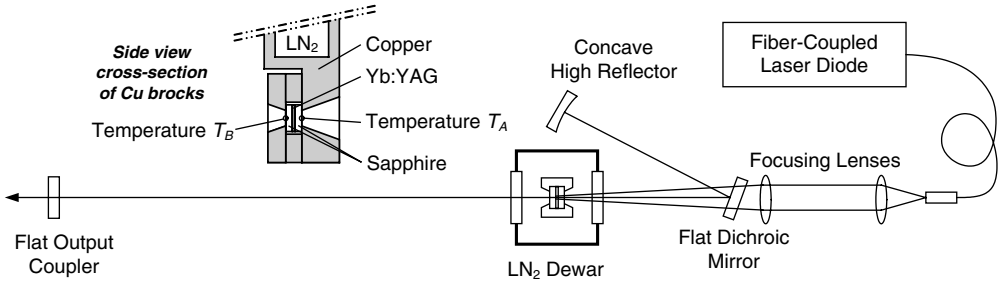

FIGURE 1 Schematic of a diode-pumped cryogenic Yb:YAG laser oscillator

and a 6 mm × 6 mm cross section. The Yb:YAG crystal was sandwiched with two sapphire crystals with a 1.6-mm thickness. The *c*-axes of the sapphire crystals were parallel to the laser propagation. The sapphire crystals were not bonded but optically contacted. Both contact surfaces of the Yb:YAG and the sapphire crystals were polished to a flatness of 1/4 wave or better (at a wavelength of 633 nm), and carefully cleaned before contacting. Since a difference of the refractive index between YAG and sapphire is small, Fresnel reflection loss at the contact surface is negligible. The reflectivity on the contact surface was measured to be approximately 0.2% with no optical coatings. The crystal sandwich was held between two copper blocks with an aperture of a 4-mm diameter in a liquid-nitrogen-cooled dewer. Indium sheets with a 100-μm thickness were squeezed between the sapphire and the copper blocks providing a good thermal contact. The side faces of Yb:YAG and sapphire crystals have no thermal contact with the copper block. Two thin thermocouples were inserted with indium sheets for measuring the temperature of the two sapphires. The two temperature measuring points are shown in Fig. 1 as T_A and T_B. The outer surfaces of the two sapphire crystals have an antireflection coating for both the pump and lasing wavelength. The copper block in one side was cooled directly by liquid nitrogen. Two fused-silica windows with antireflection coating provided the vacuum seal on the liquid-nitrogen-cooled dewer. A 600-μm-core fiber coupled laser diode was used as the cw pump source. The central wavelength of the laser diode emission was 938 nm at the maximum output power. The pump beam was focused into the Yb:YAG crystal through the dichroic mirror by two doublet lenses of focal lengths 30 and 75 mm. The spatial profile of pump beam on the Yb:YAG crystal was circular and nearly flat-top with 1.5-mm diameter. A maximum pump power was 135 W after passing the dichroic mirror. The incident pump intensity was calculated to be 7.6 kW/cm^2.

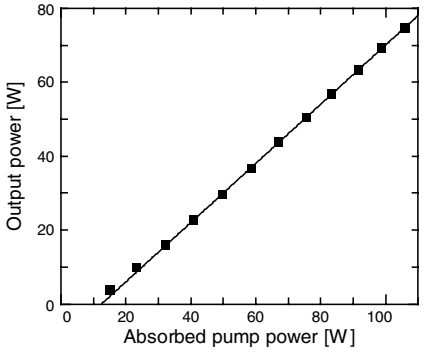

FIGURE 2 Output power as a function of absorbed pump power

3 Experimental results and thermal analysis

Figure 2 shows the output power as a function of absorbed pump power. The maximum output power was 75 W at an absorbed pump power of 106 W with an output coupler of 72% reflectivity. The slope efficiency and the maximum optical-optical efficiency were 80 and 70%, respectively, with respect to the absorbed pump power. With 135 W of incident pump power, the Yb:YAG crystal had an absorption coefficient of 25 cm^{-1}, resulting in a single-pass absorption of 78% under lasing condition. The average pump power density was calculated to be 100 kw/cm^3. The emission wavelength was always 1029 nm. The beam quality was close to the diffraction limit, with an M^2 factor measured to be <1.1 at the maximum output. An image of the output beam measured by a CCD camera and a horizontal profile is shown in Fig. 3. The output beam fits well to a Gaussian profile. In a condition with the insertion of an intracavity Brewster plate, the output power was measured as a function of the pump power for a polarized laser cavity. The differences in output power between the unpolarized and the polarized laser cavity were negligible even in the maximum pump power. These results show that the thermally induced birefringence in the laser crystal was very small. Figure 4 shows the temperatures T_A and T_B of the two measuring points as a function of the absorbed pump power under lasing and non-lasing conditions. The temperatures increased with increasing the pump power. The temperature of T_B

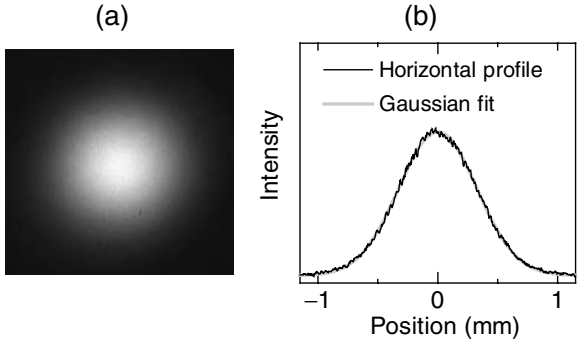

FIGURE 3 **a** Beam profile measured by CCD camera at a maximum output power. **b** Horizontal slice through center of beam profile with Gaussian fit

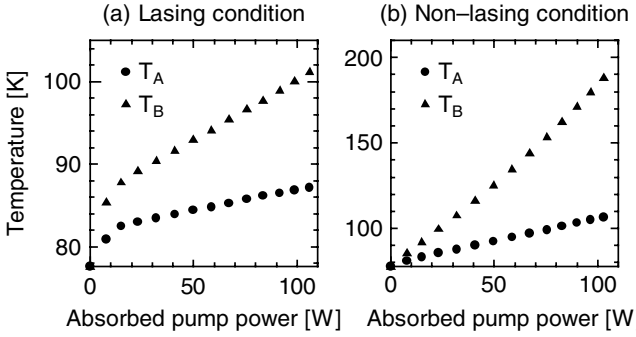

FIGURE 4 The temperatures T_A and T_B of the two measuring points as a function of absorbed pump power

was obviously higher than T_A due to the difference in the heat transference of the two copper blocks to the liquid nitrogen. Under the non-lasing condition, T_A and T_B were significantly higher than those under the lasing condition due to the heating of copper blocks induced by much stronger fluorescence.

In order to estimate the temperature in the laser active region under the lasing condition, we have numerically simulated the temperature distribution for the Yb:YAG and the sapphire crystals based on the steady-state heat diffusion equation. Using an axisymmetric approximation, the two-dimensional temperature profile for half of the axial cross section (rz plane) was calculated by the finite difference method. The thermal conductivities of Yb:YAG and sapphire crystal greatly decreased along with the temperature increase in cryogenic region. The thermal conductivities from YbAG's data in Ref. [5] and Sapphire's data in Ref. [6] were applied to the calculations as a function of temperature. The surfaces contacting to the copper block of the two sapphire crystals were assumed to be at fixed temperature as boundary conditions. The measured temperatures T_A and T_B were given as the boundary temperature. Poor thermal contact or vacuum gaps between the Yb:YAG and the sapphire may cause further temperature rises of the laser active region. The mean heat transfer coefficient of the contact surfaces was measured to be about 4×10^4 W/m^2 K by the steady-state heat-flow method. This coefficient was applied to the calculations. It was assumed that the heating source has a flat-top radial distribution and an exponentially decreasing profile along the thickness of the Yb:YAG crystal, and that 10% of the absorbed pump power was converted to heat in the pumping region.

To confirm experimentally the validity of the numerical simulation, we measured the thermal lensing and the fluorescence spectra depending on the pump power under the non-lasing condition. The thermal lens focal lengths were measured by observing a 633-nm He–Ne probe beam transmitted through the laser active region using a CCD camera. The measured and calculated thermal lens power (reciprocal of focal length) as a function of the absorbed pump power is shown in Fig. 5. The thermal lens power nonlinearly increased with the absorbed pump power due to the decreasing thermal conductivity and the increasing dn/dT. With the maximum pump power, the thermal lens focal length was measured to be about 2 m. The calculated results show good agreement with the experimental results. The calculation of the thermal lensing was performed based on the change of the refractive index with temperature in the sapphire and Yb:YAG crystals. The optical path difference along the beam radius calculated from the temperature

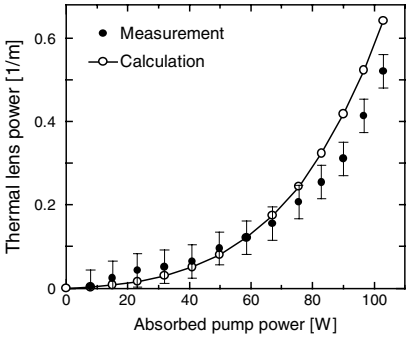

FIGURE 5 The measured and calculated thermal lens power as a function of absorbed pump power

profile was fitted to a parabolic function, and was approximated as a positive lens. The dn/dT as a function of temperature in the Refs. [7, 8] were applied to the calculations.

The fluorescence spectra from the Yb:YAG crystal were measured by a multi-channel spectrometer under the non-lasing condition. Since the florescence spectrum of Yb:YAG changes with temperature [11], the observed spectrum under high power pumping depends on the temperature profile and the fluorescence emission profile in the active medium. We simulated the observable spectral intensity ratio at wavelengths 1022 and 1027 nm from the following expression:

$$I_{ob}(\lambda) \propto \iiint_V I_{em}(\lambda, T(r,z))\rho_e(r,z)\,dV, \tag{1}$$

where T is the temperature profile in the pumping region, I_{em} is the measured spectrum with uniform temperature profile, ρ_e is the density of excited ions. The I_{em} was measured under the controlled temperature and the weak pumping conditions at 78–300 K. It was assumed that the ρ_e is similar to the pumping profile that has an exponential profile along the z-axis. Because, in the measured spectra, the spontaneous amplification was clearly observed at the strong fluorescence peak of 1029 or 1025 nm, we chose the peak at 1022 nm and the valley at 1027 nm. The measured and calculated spectral intensity ratio as a function of the absorbed pump power is shown in Fig. 6. The calculated results show good agreement with the experimental results. In this case the sensitivity of the peak temperature to the spectral intensity ratio was -0.02 to -0.06 par 10 K. The discrepancy of the intensity ratio between the measurement and the calculation resulted in the difference of the estimated peak temperature of about <8 and <25 K in lower and higher than 70-W absorbed pump power region, respectively.

Figure 7 shows the calculated peak temperature as a function of the absorbed pump power. The peak temperatures under the lasing and the non-lasing conditions with the maximum pump power were estimated to be about 170 and 250 K, respectively. In an ideal condition, that is, with no temperature

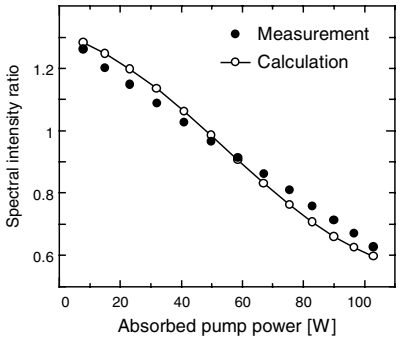

FIGURE 6 The measured and calculated spectral intensity ratio between 1022 and 1027 nm as a function of absorbed pump power

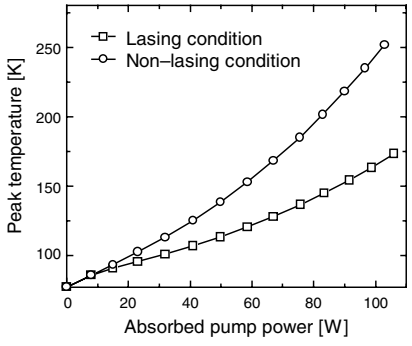

FIGURE 7 The calculated peak temperature as a function of absorbed pump power

increase in the copper blocks (fixed 78 K) and the perfect thermal contacts between the Yb:YAG and the sapphire crystals, the peak temperature with the maximum pump power was calculated to be only about 90 K. In a condition only with no temperature increase in the copper blocks, the peak temperature was calculated to be about 145 K. It is inferred that the non-perfect thermal contacts was the main cause of the considerable temperature increase in our experiments. It was calculated that the peak temperature was almost inversely proportional to the heat transfer coefficient of the contact surfaces. If the heat transfer coefficient is improved by one order of magnitude, the near-best performance will be obtained. Higher degree of flatness of the contact surfaces with 1/10th wave or better may lead to the improvement of the heat transfer. The sapphire crystals, however, played a key role in this experiment. It is noted that a 25 at.% Yb:YAG crystal with 0.8-mm thickness was thermally fractured by about 60-W absorbed pump power when not employing the sapphire cooling. In this fatal condition, it was calculated that the peak temperature was reached room temperature or higher.

4 Conclusion

We have demonstrated a high-power cryo-cooled Yb:YAG disk laser based on conduction cooling at both faces with sapphire crystals. We obtained 75-W output power with a near-diffraction-limited beam quality without any compensation for the thermal induced effects. The peak temperature of the active medium was estimated by numerical simulations. It was apparent that the non-perfect thermal contacts between the crystals caused the considerable temperature increase. Nonetheless, the high-power operation with a high pump density was achieved using a highly doped Yb:YAG crystal. A good absorption efficiency was obtained with a single path pumping by allowing to use a relatively thick active medium as compared to typical thin-disk lasers. The presented configuration would provide a good scalability for larger pump beam diameter.

REFERENCES

1 T.Y. Fan, T. Crow, B. Hoden, Proc. SPIE **3381**, 200 (1998)
2 D.J. Ripin, J.R. Ochoa, R.L. Aggarwal, T.Y. Fan, Opt. Lett. **29**, 2154 (2004)
3 P.A. Schulz, S.R. Henion, IEEE J. Quantum Electron. **27**, 1039 (1991)
4 S. Backus, R. Bartels, S. Thompson, R. Dollinger, H.C. Kapteyn, M.M. Murnane, Opt. Lett. **26**, 465 (2001)
5 G.A. Slack, D.W. Oliver, Phys. Rev. B **4**, 592 (1971)
6 M.G. Holland, J. Appl. Phys. **33**, 2910 (1962)
7 R. Wynne, J.L. Daneu, T.Y. Fan, Appl. Opt. **38**, 3282 (1999)
8 A.C. DeFranzo, B.G. Pazol, Appl. Opt. **32**, 2224 (1993)
9 J. Kawanaka, H. Nishioka, N. Inoue, K. Ueda, Appl. Opt. **40**, 3542 (2001)
10 T. Shoji, S. Tokita, J. Kawanaka, M. Fujita, Y. Izawa, Jpn. J. Appl. Phys. **43**, 496 (2004)
11 J. Dong, M. Bass, Y. Mao, P. Deng, F. Gan, J. Opt. Soc. Am. B **20**, 1975 (2003)
12 A. Giesen, H. Hügel, A. Voss, K. Wittig, U. Brauch, H. Opower, Appl. Phys. B **58**, 365 (1994)
13 E. Innerhofer, T. Südmeyer, F. Brunner, R. Häring, A. Aschwanden, R. Paschotta, C. Hönninger, M. Kumkar, U. Keller, Opt. Lett. **28**, 367 (2003)
14 F. Brunner, T. Südmeyer, E. Innerhofer, F. Morier-Genoud, R. Paschotta, V.E. Kisel, V.G. Shcherbitsky, N.V. Kuleshov, J. Gao, K. Contag, A. Giesen, U. Keller, Opt. Lett. **27**, 1162 (2002)
15 M. Larionov, J. Gao, S. Erhard, A. Giesen, K. Contag, V. Peters, E. Mix, L. Fornasiero, K. Petermann, G. Huber, J. Aus der Au, G.J. Spühler, F. Brunner, R. Paschotta, U. Keller, A.A. Lagatsky, A. Abdolvand, N.V. Kuleshov, OSA TOPS **50**, 625 (2001)
16 F. Hanson, Appl. Phys. Lett. **66**, 3549 (1995)
17 M. Tsunekane, N. Taguchi, T. Kasamatsu, H. Inaba, IEEE J. Sel. Top. Quantum Electron. **3**, 9 (1997)
18 D.C. Brown, R. Nelson, L. Billings, Appl. Opt. **36**, 8611 (1997)
19 M. Tsunekane, N. Taguchi, H. Inaba, Appl. Opt. **37**, 3290 (1998)